Volume 1 | Number 1 | Jan 2013 | Pages 1–100

ChemComm

Chemical Communications
www.rsc.org/chemcomm

ROYAL SOCIETY OF CHEMISTRY

ROYAL SOCIETY OF CHEMISTRY

www.rsc.org/chemcomm

Journal Name

ChemComm

ARTICLE TYPE

Crystallographic insight-guided nanoarchitectonics and conductivity modulation of n-type organic semiconductor through peptide conjugation†

M. Pandeeswar,[a] Harshavardhan Khare,[b] Suryanarayanarao Ramakumar,[b] and T. Govindaraju*[a]

Crystallographic insight-guided nanoarchitectonics of peptide-conjugated naphthalene diimide (NDI) is described. In a bio-inspired approach, non-proteinogenic α-amino isobutyric acid (Aib)- and alanine (Ala)-derived peptides orchestrated 1D achiral and 2D chiral molecular ordering of NDI respectively which resulted in modulation of nanoscale morphology, chiroptical and conductivity properties.

Ingenious organisation of functional aromatic molecular systems is one of the key challenges in the fields of chemistry, biology and material science.[1-2] In particular, the performance of solution-processable, flexible, organic thin-film devices is determined by the nature of solid-state molecular ordering and resultant nanoscale morphology on the substrate.[2-3] In this context, several strategies have been attempted to gain control over noncovalent interaction-driven molecular self-assembly of organic semiconductors to achieve the desired nanoscale morphology.[3] However, the art of pre-programmed molecular assembly and structure-property correlation in case of self-assembled molecular materials to facilitate development of new organic electronic devices is still in its infancy. The ideal way to investigate the structure-property correlations of molecular materials is essentially through the study of similar molecular structures that differ in their molecular ordering.[2] Theoretical calculations have predicted that on account of maximum electronic coupling, face-to-face π-π molecular ordering facilitates a higher charge carrier mobility.[2] However such prerequisite of perfect face-to-face stacked molecular organisation of organic semiconductors is seldom met in real solid-state structures.[2a]

In nature, biomolecules, specifically (poly)peptides, have built-in information to undergo highly ordered sequence-specific molecular organisation by means of synchronised noncovalent interactions to form complex biological materials with predetermined functions.[1,4] In the past few years, principles of bio-inspired engineering of molecular assemblies (molecular architectonics) has motivated the scientific community to design the assembly of functional aromatic molecules, producing nanomaterials with tunable molecular ordering for various multidisciplinary applications.[4-7]

Herein, we demonstrate the bio-inspired structure-property correlation *via* the modulation of molecular organisation of the
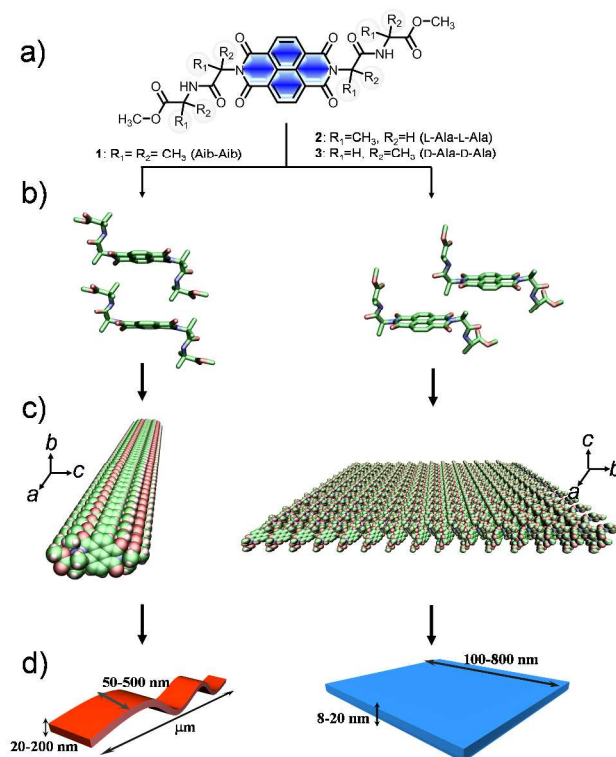

Fig. 1 (a) Molecular structures of bis-dipeptide conjugated NDIs **1**: Aib-Aib, **2**: L-Ala-L-Ala, and **3**: D-Ala-D-Ala. The solid state structural insights: (b) face-to-face (**1**) and edge-to-edge (**2**) stacked dimmers and (c) Subsequent space fill representation of 1D (**1**) and 2D (**2**) molecular ordering along the crystallographic *a*-axis and *c*-face respectively (solvent molecules and hydrogen atoms have been omitted from the crystal packing representation for clarity). (d) Schematic representation of self-assembled 1D and 2D nanostructures of **1** and **2**, respectively.

promising n-type organic semiconductor naphthalene diimide (NDI) by conjugating dipeptides. We chose to functionalise NDI with structurally comparable unnatural and natural peptides Aib-Aib (**1**) and Ala-Ala (**2** and **3**), respectively. They differ in just one additional methyl group at C_α position in case of Aib, and are capable of forming unique secondary structures, as shown in Fig. 1a and 1b. The minute structural mutations (methyl groups) are expected to influence their distinct molecular organisation. Notably, Aib-rich peptides are known to promote helix
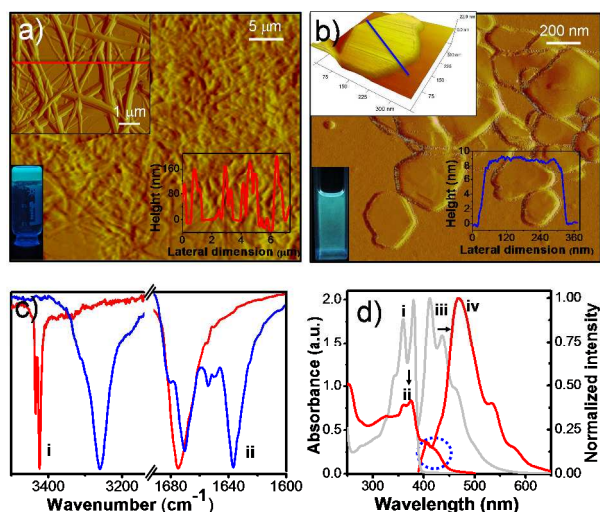
Fig. 2 AFM micrographs (amplitude image); (a) 1D nanotape network from xerogel of **1** and (b) 2D nanosheets form solution of **2**. *Insets*: (a) organogel of **1** under UV light (365 nm), a selected area AFM image of 1D nanotapes and corresponding height profiles along the red line
5 (derived from height image); (b) MCH/CHCl$_3$ (90/10, v/v) solution of **2** under UV light (365 nm), a selected area 3D AFM height image of single 2D nanosheet and corresponding height profiles along the blue line. (c) ATIR spectra of 1D nanotapes (i) and 2D nanosheets (ii). (d) UV-vis (i and ii) and fluorescence emission (iii and iv) spectra of **1** in CHCl$_3$ (gray:
10 i and iii) and MCH/CHCl$_3$ (90/10, v/v) (red: ii and iv), respectively. Arrows and blue dotted circle indicating the spectral changes and the appearance of new absorption band, respectively.

conformation while the Ala-rich peptides assist β–sheet formation, as in the case of spider silk proteins.[8] The influence of
15 structural mutations in (*bis*-dipeptide)-NDI conjugates (NDIs **1-3**) on their solid-state ordering and resultant properties *viz.*, (chiro-)optoelectronic, self-assembled nanoscale morphology and electrical conductivity was studied (Fig. 1).

To the best of our knowledge we present crystallographic
20 insight-guided distinct solid-state molecular ordering to modulate the conducting property of n-type organic semiconductor molecule NDI by peptide conjugation, for the first time. The impact of minute structural mutations in the form of peptides revealed the distinct but well-defined nanostructures (1D
25 nanotapes and 2D nanosheets) with perfect face-to-face (achiral) and edge-to-edge (chiral) NDI-NDI self-assembly, respectively (Fig 1b-d). The significance of such bio-inspired molecular architectonics[1,4-7,10a] of NDI and resultant structure-property correlation was thoroughly studied by various spectroscopic and
30 microscopy techniques.

In line with the strategy, we sought to investigate the molecular ordering of *bis*-dipeptide-conjugated NDIs **1-3** by single crystal X-ray diffraction (XRD) studies (Fig. 1b&c). The crystals of **1-3**, suitable for single crystal XRD, were grown in dimethylsulfoxide
35 (DMSO) by the slow solvent evaporation method. NDI **1** was found to crystallise in the monoclinic system with P2$_1$/n space group while NDIs **2** and **3** crystallised in orthorhombic systems with space group P2$_1$2$_1$2$_1$. Single crystal structures revealed that the imide substituents (dipeptides, **1**: Aib-Aib, **2**: L-Ala-L-Ala,
40 and **3**: D-Ala-D-Ala) in NDIs (**1-3**) adopt *trans*-conformation (i.e., peptide chains on either side of NDI oriented in opposite directions with respect to the central aromatic core) and exhibit distinct sequence-specific molecular packing (Fig 1b) (ESI†). To

our surprise, unnatural dipeptide (Aib-Aib)-conjugated NDI (**1**)
45 showed 1D molecular ordering with face-to-face NDI-NDI organisation along crystallographic *a*-axis. The face-to-face 1D orientation of NDI-core is stabilized by CH---CO (α-methyl on the peptide to acyl carbon on NDI), NH---O hydrogen bond (between peptide-NH and Oxygen atom from solvent molecule,
50 DMSO) and CH---O (between α-methyl groups on peptide and solvent molecule, DMSO) (Fig 1b&c, ESI†). In contrast, **2** and **3** displayed 2D edge-to-edge NDI-NDI molecular ordering through β–bridge-like interactions (series of CO---NH hydrogen bonds) between the peptide backbones along the crystallographic *a*-axis,
55 giving rise to a hydrogen bond network spreading across the *c*-face of the crystal lattice (Fig 1b&c, ESI†). Furthermore, **1** exhibited gelation propensity by forming bright cyan fluorescent organogel in CHCl$_3$/methylcyclohexane (MCH) (90/10 v/v) with minimum gelation concentration (MGC) of 1 mM (Fig 2a, inset).
60 On the other hand, **2** and **3** failed to form organogel under similar conditions (Fig 2b, inset). Thus, the observed distinct solid-state molecular organisation and gelation ability of *bis*-(Aib-Aib) (**1**)- and *bis*-(Ala-Ala) (**2** and **3**)-functionalised NDIs validated the importance of bio-inspired molecular architectonics to rationally
65 design molecular systems with desired molecular ordering, by utilising minute structural mutations in the form of peptide sequence.

The consequence of distinct molecular ordering on nanoscale morphology of **1** and **2** was examined by atomic force
70 microscopy (AFM) (Fig. 2a-b) and field emission scanning electron microscopy (FESEM) (ESI†). The xerogel of **1** revealed the presence of several micrometer long, high-aspect-ratio 1D tape network. AFM height profile analysis revealed 1D nanotapes with 20-200 nm height and 50-500 nm width (Fig. 2a). On the
75 other hand, **2** self-assembled from its solution (MCH/CHCl$_3$: 90/10, v/v) into thin, large surface area 2D sheets with ~ 8-20 nm thickness and 100-800 nm lateral dimensions (Fig. 2b). Thus, 1D and 2D molecular packing observed in the single crystals were found to be replicated in the self-assembled nanoscale structures
80 of **1** and **2** (Fig 1c). Attenuated total reflection infrared (ATIR) spectroscopy further provided the secondary structures of peptides and hydrogen bonding interactions among the molecules within the 1D nanotapes (**1**) and 2D nanosheets (**2**) (Fig 2c). 1D nanobelts of **1** exhibited intense amide-I ($\nu_{C=O}$) absorption band at
85 1675 cm^{-1}, indicating the random structure of Aib-Aib peptide backbone. On the other hand, Ala-Ala (**2** and **3**) displayed a strong amide-I band at 1636 cm^{-1} and a weak signal at 1682 cm^{-1}, suggesting the presence of antiparallel β-sheet like structure within the 2D nanosheets.[9] In agreement with the solid-state
90 crystal structures, 2D nanosheets (**2**) revealed the existence of strong intermolecular hydrogen bonding network *via* amide N-H and C=O by displaying blue-shifted broad amide N-H symmetric stretching band (3261 cm^{-1}) as compared to that of 1D nanobelts of **1** (3425 cm^{-1}).
95 UV-vis absorption spectrum of **1** in CHCl$_3$ exhibited vibronically well-resolved absorption bands in the 300-400 nm region, which is a characteristic of π–π* transitions along the long-axis of NDI chromophore (Fig. 2d). A mirror image emission spectrum around 413 nm (λ_{max}) suggested typical
100 monomeric state in CHCl$_3$. Interestingly, absorption spectrum of **1** in MCH/CHCl$_3$ (90/10, v/v) displayed significant

hypochromicity (~ 42%), blue-shift (~ 5 nm) and band broadening. Furthermore, a new band appeared in the longer wavelength region (415 nm). The fluorescence emission spectrum of **1** in MCH/CHCl₃ exhibited a significantly enhanced, broad and large Stoke-shifted (~ 93 nm) emission band, centred around 468 nm, with bi-exponential lifetime values of 9 ns (18%) and 1 ns (82%) (Fig. 2d, ESI†). This study suggests the formation of face-to-face (H-type) exciton-coupled NDI-NDI π−π stacked self-assembly among the molecules of **1** (Fig.1b).[10] In contrast, **2** showed red-shifted (~ 5 nm) absorption bands by changing the solvent system from CHCl₃ to MCH/CHCl₃ (90/10, v/v). Corresponding emission spectra displayed a large Stoke-shifted broad emission band centred at 522 nm with relatively shorter lifetime values of 4.9 ns (48%) and 1.3 ns (52%), thus, signifying the formation of edge-to-edge (J-type) stacked NDI-NDI self assembly.[10] These results were further strengthened by ¹H NMR data (ESI†). Due to enhanced ring current shielding in face-to-face π-stacked arrangement, a significant up-field shift ($\Delta\delta_{NDI}$= 160 ppb) was observed for NDI-core protons of **1** compared to edge-to-edge interacting NDI-core in **2**. Variable-temperature (VT) emission studies of **1** and **2** monitored at 460 nm and 522 nm, respectively, exhibited two times higher melting temperatures (50% aggregates were intact even at 75 °C) for face-to-face assembly of **1** as compared to that of edge-to-edge assembly of **2** (50% aggregates were present at 38 °C) (ESI†). The influence of MCH on the NDI-NDI aromatic stacking and hydrogen bonding interactions of **1** and **2** were probed by solvent-dependent ¹H NMR measurements. Fig. 3a clearly shows the up-field and down-field shifting of NDI-aromatic (7 ppb) (face-to-face NDI self-assembly) and peptide-amide protons (20 ppb) (solvent induced hydrogen bonding), with the increasing volume fraction of MCH in CDCl₃ solution of **1** (ESI†). Under similar conditions, **2** exhibited relatively less down-field shift (6 ppb) (β−bridge interactions) of peptide-amide protons and increased up-field shifts (8 ppb) of NDI-aromatic protons (edge-to-edge NDI self-assembly). These changes in chemical shifts suggested that the MCH facilitated distinct self-assembly among the molecules of **1** and **2** by reinforcing the noncovalent interactions *via* intermolecular NDI-NDI aromatic and hydrogen bonding among the peptide chains. Furthermore, although solvent systems used for crystal growth and nanostructures of **1** and **2** are different, the detailed spectroscopic and microscopy studies in MCH/CHCl₃ (90/10, v/v) support face-to-face (H-type) and edge-to-edge (J-type) molecular arrangements for **1** and **2** respectively (Fig 2. and Fig. S6d in ESI†), which is in good agreement with XRD data.

The effect of chiral information of peptide backbones in **2** and **3** against achiral backbone in **1** on the long-range intermolecular organisation of NDI was investigated by circular dichroism (CD) spectroscopic studies (Fig. 3b). In agreement with the UV-vis and fluorescence emission data, NDIs **1-3** displayed flat CD spectra in CHCl₃ solution due to their molecularly dissolved state (ESI†) which also confirmed the absence of any Cotton effects originating from achiral conformations of methyl (C_α) group. However, **2** and **3** in CHCl₃/MCH (90/10, v/v) displayed mirror image cotton effects in the NDI absorption region (250-400 nm). The negative and positive cotton effects of **2** and **3**, around 400 nm (NDI long axis π−π* electronic transitions), suggests left (*M*)-
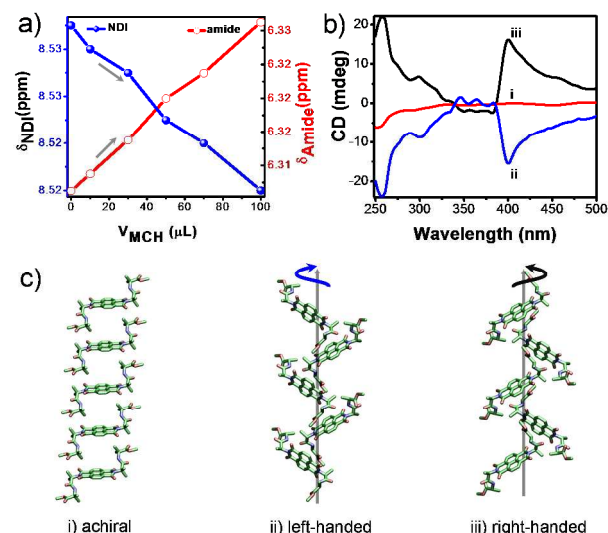

Fig. 3 (a) ¹H NMR data of **1** depicting the change in the chemical shift (ppm) values of NDI aromatic protons (blue line) and peptide-amide NH protons (red line) as a function of volume of MCH added into CDCl₃ solution. (b) CD spectra of **1** (i), **2** (ii) and **3** (iii) recorded in MCH/CHCl₃(90/10, v/v) solution. (c) Solid-state 1D face-to-face achiral organisation of **1** (i), supramolecular tilt left-handed (ii, in **2**) and right-handed (iii, in **3**) chiral NDI stacks from single crystal XRD studies.

and right (*P*)-handed supramolecular helical organisation of NDI chromophores.[5c,10a] NDI **1** with achiral and non-proteinogenic peptide (Aib-Aib) did not show CD signal under similar conditions, indicating the absence of any preferred helical assembly. To validate the CD data, we further analysed solid-state molecular organisation in the single crystal packing of **1-3** (Fig. 3c). The linear 1D face-to-face molecular stacks of **1** in the crystal lattice were found to co-exist as both left- and right-handed 2₁ chiral helices, thus nullifying the chiral signature in the CD spectra. On the other hand, **2** and **3** showed prominent 2₁ supramolecular tilt stacks with opposite helical assembly along the crystallographic *a* and *b*-axis. In the case of **2**, the tilt angles were found to be 30.67˚ and 59.79˚ along *a* and *b*-axis, respectively. Similarly, in the case of **3**, the tilt angles were found to be 30.56˚ and 59.93˚ along *a* and *b*-axis, respectively.[5c,10a] The pitch of the helices was found to be 9.94 Å (along *a-axis*) and 14.41 Å (along *b-axis*) for **2**, while for **3** the pitch was 9.99 Å (along *a-axis*) and 14.47 Å (along *b-axis*) (ESI†). The helices were found to be stabilised by β−bridge like intermolecular CO---NH hydrogen bonding between the peptide backbones. Overall, achiral (**1**) and chiral (**2** and **3**) organisation of *bis*-dipeptide-conjugated NDIs, within the lattices of their respective crystals (Fig. 3c), is in excellent agreement with the CD data (Fig. 3b). These results further corroborated the transcription of chiral information of intrinsically chiral amino acid (alanine) of the peptide backbones in **2** and **3** to their supramolecular homochiral organisation in solution and solid state.[3c,5c,10a]

Furthermore, we examined the effect of minute structural mutations (dipeptide) guided distinct NDI molecular organization of **1** (1D face-face) and **2** (2D edge-edge) on the charge carrier mobility (Fig 4). Two-probe method was employed to generate the current-voltage (I-V) response from the films of **1** (1D nanotapes) and **2** (2D sheets) as shown in Fig. 4a. Remarkably,
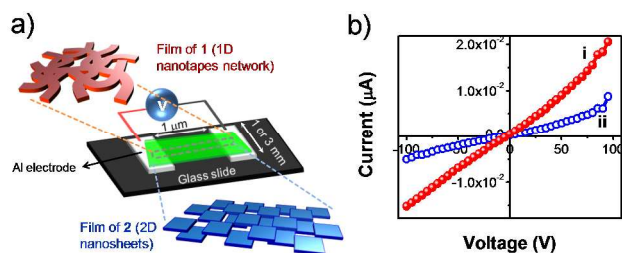
Fig. 4 (a) Schematic representation of current-voltage (*I-V*) device fabricated using nanotapes network film from xerogel of **1** or 2D nanosheets film from **2** nanostructured materials of NDI. (b) *I-V* characteristics of **1** (1D nanotapes network) (i) and **2** (2D nanosheets) (ii)
5 deposited across the aluminium electrodes as shown in (a).

the current-voltage (*I-V*) measurements on NDI **1** (1D nanotapes) with face-to-face NDI organisation showed two-times more conductivity (3.5 ×10⁻⁶ S/m) as compared to NDI **2** (2D nanosheets) with edge-to-edge NDI organisation (1.6 ×10⁻⁶ S/m).
10 Similar *I-V* characteristics was observed for film of **3** (2D nanosheets) which confirmed that chirality has no role in the modulation of conductivity in our peptide conjugated NDIs. The significantly enhanced conductivity of **1** is attributed to perfect face-to-face molecular arrangement, which is known to maximise
15 the electronic coupling among the π–π overlapped NDI molecules.[2] Therefore, difference in the conductivity values of NDI chromophore in 1D nanotapes of **1** and 2D nanosheets of **2** further exemplifies the potential of bio-inspired molecular architectonics guided by the crystallographic insights for the
20 modulation of functional properties (*viz.*, nanoscale morphology, (chiro-)optical and conductivity) of electronically active aromatic systems.

In conclusion, we demonstrated the crystallographic insight-guided structure-property correlation in the form of
25 nanomorphology, optoelectronic and conductivity behaviour of *bis*-dipeptide-conjugated naphthalene diimides (NDI). In our bio-inspired design strategy, minute structural mutations played a significant role in the modulation of functional properties of n-type organic semiconductor (NDI). The non-proteinogenic
30 (achiral) dipeptide (Aib-Aib) promoted 1D face-to-face arrangement (H-type) while the proteinogenic (chiral) dipeptide (Ala-Ala) led to the formation of 2D edge-to-edge (J-type) supramolecular tilted chiral molecular organisation in solid state. The molecular ordering in both single crystals and self-assembled
35 nanostructures (1D and 2D) showed unusually high correlations, which reflected in their distinct optoelectronic and conductivity properties. Thus, our report on crystallographic insight-guided and bio-inspired molecular architectonics is not only envision novel way of engineering molecular assemblies and to undertake
40 structure-property correlations but it may also facilitate the interfacing of the electronic materials with biology to enable many advanced biomaterial (bioelectronics) applications.

Notes and references

aBioorganic Chemistry Laboratory, New Chemistry Unit, Jawaharlal Nehru Centre for Advanced Scientific Research, Jakkur P.O., Bengaluru 560064, India. Fax: (+) 91 80 22082627; E-mail: tgraju@jncasr.ac.in

50 *bDepartment of Physics, Indian Institute of Science, Bengaluru-560012, India.*

60 1 a) L. M. Salonen, M. Ellermann and F. Diederich, *Angew. Chem. Int. Ed.*, 2011, **50**, 4808-4842; b) K. E. Riley and P. Hobza, *Acc. Chem. Res.*, 2013, **46**, 927-936; c) M. B. Avinash and T. Govindaraju, *Nanoscale*, 2014, **6**, 13348-13369; d) K. Ariga, K. Kawakami, M. Ebara, Y. Kotsuchibashi, Q. Ji and J. P. Hill, *New J. Chem.*, 2014, **38**,
65 5149-5163; e) K. Ariga, Q. Ji, W. Nakanishi, J. P. Hill and M. Aono, *Mater. Horiz.*, 2015, DOI: 10.1039/C1035MH00012B.

2 a) V. Coropceanu, J. Cornil, D. A. da Silva Filho, Y. Olivier, R. Silbey and J.-L. Brédas, *Chem. Rev.*, 2007, **107**, 926-952; b) M.; Mas-Torrent and C. Rovira, *Chem. Rev.*, 2011, **111**, 4833-4856.

70 3 a) K. Sakakibara, J. P. Hill and K. Ariga, *Small*, 2011, **7**, 1288-1308; b) T. Aida, E. W. Meijer and S. I. Stupp, *Science*, 2012, **335**, 813−817; c) M. Pandeeswar and T. Govindaraju, *RSC Adv.* 2013, **3**, 11459-11462; d) Y. Diao, L. Shaw, Z. Bao and S. C. B. Mannsfeld, *Energy Environ. Sci.*, 2014, 7, 2145-2159. e) K. Ariga, Y. Yamauchi,
75 G. Rydzek, Q. Ji, Y. Yonamine, K. C. W. Wu and J. P. Hill, *Chem. Lett.*, 2014, **43**, 36-68; f) X. Cheng, S. B. Lowe, P. J. Reece and J. J. Gooding, *Chem. Soc. Rev.*, 2014, **43**, 2680-2700.

4 a) K. Ariga, J.-i. Kikuchi, M. Naito, E. Koyama and N. Yamada, Langmuir, 2000, 16, 4929-4939; b) S. Ghosh, M. Reches, E. Gazit
80 and S. Verma, *Angew. Chem. Int. Ed.*, 2007, **46**, 2002-2004; c) A. Jatsch, E. K. Schillinger, S. Schmid and P. Bauerle, *J. Mater. Chem.*, 2010, **20**, 3563-3578; d) M. B. Avinash and T. Govindaraju, *Adv. Mater.*, 2012, **24**, 3905- 3922. e) T. Govindaraju and M. B. Avinash, *Nanoscale*, 2012, **4**, 6102-6117; f) M. B. Avinash, P. K. Samanta, K.
85 V. Sandeepa, S. K. Pati and T. Govindaraju, *Eur. J. Org. Chem.,* 2013, 5838-5847.

5 a) N. Ashkenasy, W. S. Horne and M. R. Ghadiri, *Small*, 2006, **2**, 99-102; b) S. H. Kim and J. R. Parquette, *Nanoscale*, 2012, **4**, 6940-6947;c) M. Pandeeswar, M. B. Avinash and T. Govindaraju, *Chem.*
90 *Eur. J.*, 2012, **18**, 4818-4822; d) J. D. Tovar, *Acc. Chem. Res.*, 2013, **46**, 1527-1537; e) U. Lewandowska, W. Zajaczkowski, L. Chen, F. Bouillière, D. Wang, K. Koynov, W. Pisula, K. Müllen and H. Wennemers, *Angew. Chem. Int. Ed.*, 2014, **53**, 12537-12541.

6 a) R. J. Kumar, J. M. MacDonald, T. B. Singh, L. J. Waddington and
95 A. B. Holmes, *J. Am. Chem. Soc.*, 2011, **133**, 8564-8573; b) C. Peebles, R. Piland and B. L. Iverson, *Chem. Eur. J.*, 2013, **19**, 11598-11602; c) S. K. M. Nalluri, C. Berdugo, N. Javid, P. W. J. M. Frederix and R. V. Ulijn, *Angew. Chem. Int. Ed.*, 2014, **53**, 5882–5887.

100 7 a) G. D. Pantoş, P. Pengo and J. K. M. Sanders, *Angew. Chem. Int. Ed.*, 2007, **46**, 194-197; b) A. K. Dwivedi, M. Pandeeswar and T. Govindaraju, *ACS Appl. Mater. Interfaces*, 2014, **6**, 21369-21379; c) M. Pandeeswar and T. Govindaraju, *J Inorg Organomet Polym*, 2015, 25, 293-300.

105 8 a) R. Nagaraj and P. Balaram, *Acc. Chem. Res.*, 1981, **14**, 356-362.b) P. Calvert, *Nature*, 1998, **393**, 309-311.

9 a) C. Toniolo and M. Palumbo, Biopolymers, 1977, **16**, 219–224; b) A. Barth, *Biochimica et Biophysica Acta*, 2007, **1767**, 1073-1101.

10 a) M. Pandeeswar, H. Khare, S. Ramakumar and T. Govindaraju, *RSC*
110 *Adv.*, 2014, **4**, 20154-20163; b) Y. Wu, M. Frasconi, D. M. Gardner, P. R. McGonigal, S. T. Schneebeli, M. R. Wasielewski and J. F. Stoddart, *Angew. Chem. Int. Ed.*, 2014, **53**, 9476-9481.

115

TOC

Crystallographic insight-guided and bio-inspired molecular nanoarchitectonics of n-type organic semiconductor is described to understand the structure-property correlation, for modulation ₅ of functional properties. The minute structural mutations in the form of *bis*-dipeptides orchestrated tunable molecular ordering, nanoscale morphology, chiroptical and conductivity properties.